11788 *Inorg. Chem.* **2009**, *48*, 11788–11798
DOI: 10.1021/ic901878h

Inorganic Chemistry
Article

Structural and Spectroscopic Studies of the PCP-Bridged Heavy Chalcogen-Centered Monoanions $[HC(PPh_2E)(PPh_2)]^-$ (E = Se, Te) and $[HC(PR_2E)_2]^-$ (E = Se, Te, R = Ph; E = Se, R = ^{i}Pr): Homoleptic Group 12 Complexes and One-Electron Oxidation of $[HC(PR_2Se)_2]^-$

Jari Konu,[†] Heikki M. Tuononen,[‡] and Tristram Chivers*[,†]

[†]*Department of Chemistry, University of Calgary, 2500 University Drive N.W., Calgary, Alberta T2N 1N4, Canada and* [‡]*Department of Chemistry, University of Jyväskylä, P.O. Box 35, Jyväskylä FI-40014, Finland*

Received September 22, 2009

Selenium- and tellurium-containing bis(diphenylphosphinoyl)methane monoanions were prepared by oxidation of the anion $[HC(PPh_2)_2]^-$ with elemental chalcogens. The selenium-containing isopropyl derivative was synthesized by generating $[H_2C(P^iPr_2)_2]$ via a reaction between $[H_2C(PCl_2)_2]$ and 4 equiv of ^{i}PrMgCl prior to in situ oxidation with selenium followed by deprotonation with LiN^iPr_2. The solid-state structures of the lithium salts of the monochalcogeno anions TMEDA·Li[$HC(PPh_2E)(PPh_2)$] (E = Se (Li**7a**), E = Te (Li**7b**)) and the dichalcogeno anions TMEDA·Li[$HC(PR_2Se)_2$] (R = Ph (Li**8a**), ^{i}Pr (Li**8c**)) revealed five- and six-membered LiEPCP and LiSePCPSe rings, respectively. The homoleptic group 12 complexes $\{M[HC(PPh_2Se)_2]_2\}$ (M = Zn (**9a**), Hg (**9b**)) were prepared from Li**8a** and MCl_2 and shown to have distorted-tetrahedral structures; the nonplanarity of the carbon center in the PC(H)P unit of the Zn complex **9a** is attributed to crystal-packing effects. The complexes Li**7a**, Li**7b**, Li**8a**, TMEDA·Li[$HC(PPh_2Te)_2$] (Li**8b**), Li**8c**, **9a**, and **9b** were characterized in solution by multinuclear (^{1}H, ^{7}Li, ^{13}C, ^{31}P, ^{77}Se, ^{125}Te, and ^{199}Hg) NMR spectroscopy. One-electron oxidation of Li**8a** and Li**8c** with iodine in a variety of organic solvents produced $[H_2C(PR_2Se)_2]$ (R = ^{i}Pr, Ph) as the final product, presumably owing to hydrogen abstraction from the solvent. DFT calculations revealed a significant contribution from the p orbital on carbon to the SOMO of the radicals $[HC(PR_2Se)_2]^•$ (R = ^{i}Pr, Ph).

Introduction

Monochalcogeno- and dichalcogenoimidodiphosphinate monoanions, $[N(PR_2E)(PR_2)]^-$ (**1**) and $[N(PR_2E)_2]^-$ (**2**) (R = ^{i}Pr, ^{t}Bu, Ph; E = S, Se, Te), are versatile acyclic ligands that have attracted considerable interest over the last few decades.[1,2] While the monochalcogeno ligands **1** and the sulfur- and selenium-containing dichalcogeno ligands **2** are readily prepared by deprotonating the neutral precursors,[1,3] the synthesis of the tellurium congener **2** requires generation of the $P^{III}NP^{III}$ anion $[N(PR_2)_2]^-$ prior to oxidation with the elemental chalcogen.[4]

Of particular interest is the recent utilization of the *dichalcogeno*imidodiphosphinate monoanions **2** (E = S, Se, Te; R = ^{i}Pr, ^{t}Bu) in redox reactions that have revealed new and unanticipated aspects of the fundamental chemistry of these well-studied anions. One-electron oxidation with iodine produces the neutral dimers $[EPR_2NR_2PE-EPR_2NR_2PE]$ (**3a**), formally involving the association of two $[EPR_2NR_2PE]^•$ radicals with elongated central E−E bonds.[5,6] Intriguingly, in addition to the neutral form **3a** these dimers can also exist as contact ion pairs where the $[N(PR_2E)_2]^-$ anion exhibits either an acyclic monodentate (**3b**) or E,E′-chelated (**3c**) coordination to one of the chalcogens of the incipient cyclic cation $[N(PR_2E)_2]^+$; the calculated energy differences between the forms **3a**−**c** are small especially when E = S, Se.[5,6]

*To whom correspondence should be addressed. E-mail: chivers@ucalgary.ca. Fax: +1 403 289 9488. Tel: +1 403 220 5741.

(1) For recent reviews on metal complexes of sulfur and selenium-centered ligands, see: (a) Haiduc, I. In *Comprehensive Coordination Chemistry II*; McCleverty, J. A., Meyer, T. J., Eds.; Elsevier: Amsterdam, 2003; pp 323−347. (b) Silvestru, C.; Drake, J. E. *Coord. Chem. Rev.* **2001**, *223*, 117. (c) Ly, T. Q.; Woollins, J. D. *Coord. Chem. Rev.* **1998**, *176*, 451.

(2) For reviews on the chemistry of tellurium-centered ligands, see: (a) Chivers, T.; Konu, J.; Ritch, J. S.; Copsey, M. C.; Eisler, D. J.; Tuononen, H. M. *J. Organomet. Chem.* **2007**, *692*, 2658. (b) Ritch, J. S.; Chivers, T.; Afzaal, M.; O'Brien, P. *Chem. Soc. Rev.* **2007**, *36*, 1622.

(3) Ritch, J. S.; Chivers, T. *Dalton Trans.* **2008**, 957.

(4) (a) Briand, G. G.; Chivers, T.; Parvez, M. *Angew. Chem., Int. Ed.* **2002**, *41*, 3468. (b) Chivers, T.; Eisler, D. J.; Ritch, J. S. *Dalton Trans.* **2005**, 2675.

(5) Chivers, T.; Eisler, D. J.; Ritch, J. S.; Tuononen, H. M. *Angew. Chem., Int. Ed.* **2005**, *44*, 4953.

(6) (a) Chivers, T.; Eisler, D. J.; Ritch, J. S.; Tuononen, H. M. *Chem. Eur. J.* **2007**, *13*, 4643. (b) Robertson, S. D.; Chivers, T.; Tuononen, H. M. *Inorg. Chem.* **2008**, *47*, 10634. (c) Robertson, S. D.; Chivers, T.; Tuononen, H. M. *Inorg. Chem.* **2009**, *48*, 6755.

Published on Web 11/20/2009

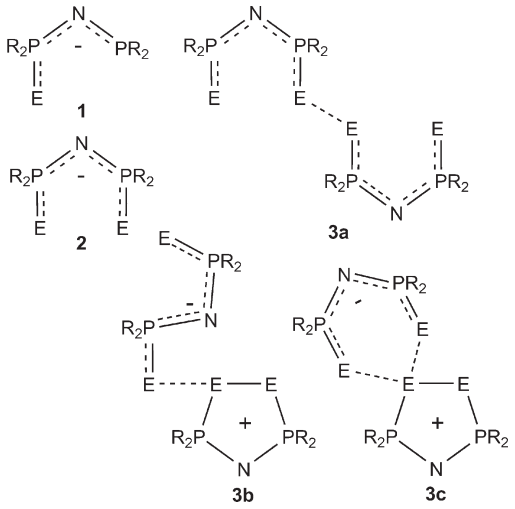

Furthermore, the formally six-π-electron five-membered cations $[N(PR_2E)_2]^+$ (E = S, Se, Te; R = ^{i}Pr, ^{t}Bu) are obtained as iodide salts by two-electron oxidation of the corresponding anions (**2**).[6a,7] In contrast, the oxidation of the phenyl-substituted derivatives $[N(PPh_2E)_2]^-$ (E = Se, Te) with 1 equiv of iodine was found to be chalcogen-dependent; the five-membered ring $[N(PPh_2Te)_2]^+$ was obtained for tellurium, whereas the unusual six-membered ring $[N(PPh_2Se)_2(\mu\text{-Se})]^+$ was the major product in the case of selenium.[7b]

These intriguing and diverse results redirected our attention to the oxidative behavior of the isoelectronic, sulfur-containing $[C(PPh_2S)_2]^{2-}$ dianion (**4**), which is prepared from $[H_2C(PPh_2S)_2]$ by treatment with 2 equiv of methyllithium.[8] In this context, we recently reported that the two-electron oxidation of the dianion **4** with iodine results in the formation of the remarkably stable dicarbenoid $[(Et_2O)(\mu\text{-Li})][(\mu_4\text{-Li})\{IC(PPh_2S)_2\}_2]$ (**5**).[9] In the absence of the combination of LiI with the initially formed $[:C(PPh_2S)_2]$ carbene, the novel, unsaturated six-membered $C_2P_2S_2$ ring in $[(SPh_2P)_2C_2(PPh_2)_2S_2]$ (**6**) is obtained.[9] Prior to our study, Le Floch and co-workers had noted that the mild oxidation of Li_2**4** with hexachloroethane produces a monomeric form of **5**: i.e., $[ClC(PPh_2S)_2]Li(OEt_2)_2$.[10]

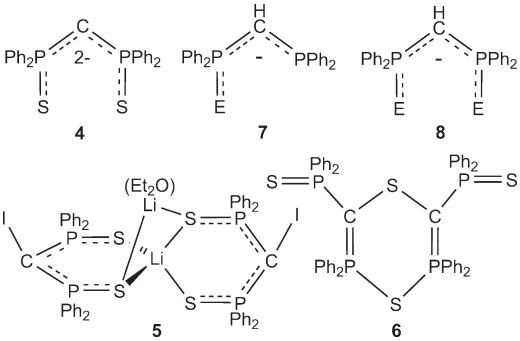

While the sulfur-containing dianion **4** has attracted considerable interest lately, primarily due to the exciting work of Le Floch et al.,[8−11] the heavier chalcogen (Se, Te) analogues of **4** have not been reported. Furthermore, even information on the related monoanions $[HC(PPh_2E)(PPh_2)]^-$ (**7**; E = Se, Te) and $[HC(PPh_2E)_2]^-$ (**8**; E = Se, Te) is sparse. The former are isoelectronic with the monochalcogenoimidodiphosphinate anions **1**, while the dichalcogeno anions **8** are isoelectronic with the monoanions **2** and the dianion **4**. A search of the Cambridge Crystallographic Database revealed only two complexes of **7** or **8**: viz., the group 14 monoseleno compound $\{Ge[(Me_3Si)C(PMe_2)(PMe_2Se)]_2\}$[12] and the diseleno complex $\{Cp^*Rh[HC(PPh_2Se)_2]ClO_4\}$,[13] in which the rhodium center is connected to the anionic PCP carbon. No solid-state structures of complexes of the tellurium-containing anions **7** and **8** (E = Te) or their neutral precursors have been reported.

In this contribution we report the synthesis, spectroscopic and structural characterization of the lithium salts TMEDA·Li[HC(PPh$_2$E)(PPh$_2$)] (E = Se (Li**7a**); E = Te (Li**7b**)) and TMEDA·Li[HC(PPh$_2$E)$_2$] (E = Se (Li**8a**), Te (Li**8b**)). In addition, we describe a one-step reaction to generate the isopropyl derivative of the PCP ligand, $[H_2C(P^iPr_2)_2]$, for the subsequent production of TMEDA·Li[HC(P^{i}Pr$_2$Se)$_2$] (Li**8c**). The utility of Li**8a** as a metathetical reagent is demonstrated by the preparation of the homoleptic group 12 complexes $\{M[HC(PPh_2Se)_2]_2\}$ (M = Zn (**9a**); Hg (**9b**)) which were structurally characterized. The one-electron oxidation of Li**8a** and Li**8c** with iodine was investigated for comparison with the analogous reactions reported for the PNP-bridged monoanions **2** (vide supra). DFT calculations were carried out in order to explain the different behavior of the transient radicals $[HC(PR_2Se)_2]^\bullet$ (**10a**, R = Ph; **10c**, R = ^{i}Pr) (hydrogen abstraction) compared to that of $[N(PR_2Se)_2]^\bullet$ (R = ^{i}Pr, ^{t}Bu) (dimerization).[5,6]

Experimental Section

Reagents and General Procedures. All reactions and the manipulations of products were performed under an argon atmosphere by using standard Schlenk techniques or in an inert-atmosphere glovebox. The compounds $[H_2C(PPh_2)_2]$ (Aldrich, 97%), $[H_2C(PCl_2)_2]$ (Strem Chemicals, >90%), ^{i}PrMgCl (Aldrich, 2.0 M solution in THF), TMEDA (Aldrich, 99%), MeLi (Aldrich, 1.6 M solution in Et_2O), $ZnCl_2$ (Acros Organics, 99.99%), and $HgCl_2$ (Strem Chemicals, 99+%) were used as received. TMEDA·Li[HC(PPh$_2$)$_2$] was prepared by the reaction between $H_2C(PPh_2)_2$ and MeLi in the presence of TMEDA in Et_2O.[14] The solvents *n*-hexane, toluene, Et_2O, and THF were dried by distillation over Na/benzophenone under an argon atmosphere prior to use. Elemental analyses were performed by Analytical Services, Department of Chemistry, University of Calgary.

(6) (a) Chivers, T.; Eisler, D. J.; Ritch, J. S.; Tuononen, H. M. *Chem. Eur. J.* **2007**, *13*, 4643. (b) Robertson, S. D.; Chivers, T.; Tuononen, H. M. *Inorg. Chem.* **2008**, *47*, 10634. (c) Robertson, S. D.; Chivers, T.; Tuononen, H. M. *Inorg. Chem.* **2009**, *48*, 6755.

(7) (a) Konu, J.; Chivers, T.; Tuononen, H. M. *Chem. Commun.* **2006**, 1634. (b) Konu, J.; Chivers, T.; Tuononen, H. M. *Inorg. Chem.* **2006**, *45*, 10678.

(8) (a) Cantat, T.; Mézailles, N.; Ricard, L.; Jean, Y.; Le Floch, P. *Angew. Chem., Int. Ed.* **2004**, *43*, 6382. (b) Cantat, T.; Ricard, L.; Jean, Y.; Le Floch, P.; Mézailles, N. *Organometallics* **2006**, *25*, 4965.

(9) Konu, J.; Chivers, T. *Chem. Commun.* **2008**, 4995.

(10) Cantat, T.; Jacques, X.; Ricard, L.; Le Goff, X.-F.; Mézailles, N.; Le Floch, P. *Angew. Chem., Int. Ed.* **2007**, *46*, 5947.

(11) (a) Blug, M.; Heuclin, H.; Cantat, T.; Le Goff, X.-F.; Mezailles, N.; Le Floch, P. *Organometallics* **2009**, *28*, 1969. (b) Cantat, T.; Arliguie, T.; Noel, A.; Thuery, P.; Ephritikhine, M.; Le Floch, P.; Mezailles, N. *J. Am. Chem. Soc.* **2009**, *131*, 963. (c) Cantat, T.; Mezailles, N.; Auffrant, A.; Le Floch, P. *Dalton Trans.* **2008**, 1957. (d) Cantat, T.; Ricard, L.; Mezailles, N.; Le Floch, P. *Organometallics* **2006**, *25*, 6030. (e) Cantat, T.; Jaroschik, F.; Nief, F.; Ricard, L.; Mezailles, N.; Le Floch, P. *Chem. Commun.* **2005**, 5178. (f) Cantat, T.; Demange, M.; Mezailles, N.; Ricard, L.; Jean, Y.; Le Floch, P. *Organometallics* **2005**, *24*, 4838.

(12) Karsch, H. H.; Baumgartner, G.; Gamper, S.; Lachmann, J.; Muller, G. *Chem. Ber.* **1992**, *125*, 1333.

(13) Valderrama, M.; Contreras, R.; Bascunan, M. *Polyhedron* **1994**, *13*, 1101.

(14) Brauer, D. J.; Hietkamp, S.; Stelzer, O. *J. Organomet. Chem.* **1986**, *299*, 137.

Table 1. Crystallographic Data for Li**7a**, Li**7b**, Li**8a**, Li**8c**, **9a**, and **9b**[a]

	Li**7a**	Li**7b**	Li**8a**	Li**8c**	**9a**	**9b**
emp formula	$C_{31}H_{37}LiN_2P_2Se$	$C_{31}H_{37}LiN_2P_2Te$	$C_{31}H_{37}LiN_2P_2Se_2$	$C_{19}H_{45}LiN_2P_2Se_2$	$C_{50}H_{42}P_4Se_4Zn$	$C_{50}H_{42}HgP_4Se_4$
fw	585.47	634.11	664.43	528.37	1147.93	1283.15
cryst syst	monoclinic	monoclinic	orthorhombic	triclinic	monoclinic	triclinic
space group	$P2_1/c$	$P2_1/c$	$Pna2_1$	$P\bar{1}$	$C2/c$	$P\bar{1}$
a, Å	8.859(2)	8.915(2)	19.730(4)	10.329(2)	26.195(5)	10.354(2)
b, Å	19.149(4)	19.407(4)	17.919(4)	11.919(2)	11.379(2)	14.489(3)
c, Å	18.131(4)	18.249(4)	9.025(2)	12.019(2)	18.610(4)	16.695(3)
α, deg	90.00	90.00	90.00	93.99(3)	90.00	111.45(2)
β, deg	100.31(3)	99.91(3)	90.00	95.60(3)	122.58(3)	94.92(3)
γ, deg	90.00	90.00	90.00	112.56(3)	90.00	93.71(3)
V, Å^3	3026(1)	3110(1)	3191(1)	1350.5(5)	4674(2)	2310.0(9)
Z	4	4	4	2	4	2
T, °C	−100	−100	−100	−100	−100	−100
ρ_{calcd}, g/cm^3	1.285	1.354	1.383	1.299	1.631	1.845
μ(Mo Kα), mm^{-1}	1.368	1.080	2.440	2.862	3.812	6.656
cryst size, mm^3	0.48 × 0.40 × 0.28	0.20 × 0.12 × 0.10	0.12 × 0.08 × 0.06	0.32 × 0.28 × 0.24	0.24 × 0.20 × 0.16	0.20 × 0.04 × 0.02
F(000)	1216	1288	1352	548	2272	1236
θ range, deg	2.98−25.03	3.35−25.03	2.27−25.02	2.86−25.03	2.87−25.02	2.37−25.03
no. of rflns collected	10 492	10 112	5409	8815	14 646	15 466
no. of unique rflns	5341	5481	5409	4743	4109	8106
R_{int}	0.0227	0.0426	0.0436	0.0266	0.0381	0.0525
no. of rflns ($I > 2\sigma(I)$)	4594	4004	4239	4253	3780	6502
R1 ($I > 2\sigma(I)$)[b]	0.0265	0.0345	0.0460	0.0323	0.0241	0.0554
wR2 (all data)[c]	0.0656	0.0717	0.0911	0.0841	0.0603	0.1389
GOF on F^2	1.029	1.015	1.065	1.064	1.066	1.061
completeness	0.997	0.996	0.996	0.993	0.998	0.993

[a] λ(Mo Kα) = 0.710 73 Å. [b] $R1 = \sum||F_o| - |F_c||/\sum|F_o|$. [c] $wR2 = [\sum w(F_o^2 - F_c^2)^2/\sum wF_o^4]^{1/2}$.

Spectroscopic Methods. The ^{1}H, ^{7}Li, ^{13}C, ^{31}P, ^{77}Se, ^{125}Te, and ^{199}Hg NMR spectra were obtained in d_8-THF at 23 °C on a Bruker DRX 400 spectrometer operating at 399.46, 155.24, 100.46, 161.71, 76.17, 125.90, and 71.49 MHz, respectively. ^{1}H and ^{13}C spectra are referenced to the solvent signal and the chemical shifts are reported relative to $(CH_3)_4Si$. ^{7}Li and ^{31}P NMR spectra are referenced externally, and the chemical shifts are reported relative to a 1.0 M solution of LiCl in D_2O and to an 85% solution of H_3PO_4. Similarly, the ^{77}Se, ^{125}Te, and ^{199}Hg NMR spectra are reported relative to neat Me_2Se, Me_2Te, and Me_2Hg, respectively.

The X-band EPR spectra were recorded on a Bruker EMX 113 spectrometer equipped with a variable-temperature accessory.

X-ray Crystallography. Crystallographic data for Li**7a**, Li**7b**, Li**8a**, Li**8c**, **9a**, and **9b** are summarized in Table 1 (see also the Supporting Information). Crystals of TMEDA·Li[HC(PPh$_2$Se)(PPh$_2$)] (Li**7a**), TMEDA·Li[HC(PPh$_2$Te)(PPh$_2$)] (Li**7b**), TMEDA·Li[HC(PPh$_2$Se)$_2$] (Li**8a**), TMEDA·Li[HC(P^{i}Pr$_2$Se)$_2$] (Li**8c**), {Zn[HC(PPh$_2$Se)$_2$]$_2$} (**9a**), and {Hg[HC(PPh$_2$Se)$_2$]$_2$} (**9b**) were coated with Paratone 8277 oil and mounted on a glass fiber. Diffraction data were collected on a Nonius KappaCCD diffractometer using monochromated Mo Kα radiation (λ = 0.710 73 Å) at −100 °C. The data sets were corrected for Lorentz and polarization effects, and an empirical absorption correction was applied to the net intensities. The structures were solved by direct methods using SHELXS-97 and refined using SHELXL-97.[15,16] After full-matrix least-squares refinement of the non-hydrogen atoms with anisotropic thermal parameters, the hydrogen atoms were placed in calculated positions (C−H = 0.95 Å for −CH, 0.99 Å for −CH$_2$, and 0.98 Å for −CH$_3$ hydrogens). The isotropic thermal parameters of the hydrogen atoms were fixed at 1.2 times that of the corresponding carbon for −CH and −CH$_2$ hydrogens and 1.5 times for −CH$_3$ hydrogens. In the final refinement the hydrogen atoms were riding on their respective carbon atoms. In the structure of Li**7b** the hydrogen atom bonded to the PCP carbon was located from the Fourier density map and it was refined.

Computational Details. Theoretical calculations on the neutral radicals **10** were done with the Gaussian 03 program using density functional theory.[17] Molecular structures were optimized with the hybrid PBE1PBE exchange-correlation functional[18] together with the Ahlrichs TZVP basis sets.[19] Hyperfine coupling constants were then calculated by single-point calculations employing the optimized structures and the basis set combination used for the optimizations. The orbital plots were obtained by the program gOpenMol.[20]

(15) (a) Sheldrick, G. M. *SHELXS-97, Program for Crystal Structure Determination*; University of Göttingen, Göttingen, Germany, **1997**.

(16) Sheldrick, G. M. *SHELXL-97, Program for Crystal Structure Refinement*; University of Göttingen, Göttingen, Germany, **1997**.

(17) Frisch, M. J.; Trucks, G. W.; Schlegel, H. B.; Scuseria, G. E.; Robb, M. A.; Cheeseman, J. R.; Montgomery, J. A., Jr.; Vreven, T.; Kudin, K. N.; Burant, J. C.; Millam, J. M.; Iyengar, S. S.; Tomasi, J.; Barone, V.; Mennucci, B.; Cossi, M.; Scalmani, G.; Rega, N.; Petersson, G. A.; Nakatsuji, H.; Hada, M.; Ehara, M.; Toyota, K.; Fukuda, R.; Hasegawa, J.; Ishida, M.; Nakajima, T.; Honda, Y.; Kitao, O.; Nakai, H.; Klene, M.; Li, X.; Knox, J. E.; Hratchian, H. P.; Cross, J. B.; Bakken, V.; Adamo, C.; Jaramillo, J.; Gomperts, R.; Stratmann, R. E.; Yazyev, O.; Austin, A. J.; Cammi, R.; Pomelli, C.; Ochterski, J. W.; Ayala, P. Y.; Morokuma, K.; Voth, G. A.; Salvador, P.; Dannenberg, J. J.; Zakrzewski, V. G.; Dapprich, S.; Daniels, A. D.; Strain, M. C.; Farkas, O.; Malick, D. K.; Rabuck, A. D.; Raghavachari, K.; Foresman, J. B.; Ortiz, J. V.; Cui, Q.; Baboul, A. G.; Clifford, S.; Cioslowski, J.; Stefanov, B. B.; Liu, G.; Liashenko, A.; Piskorz, P.; Komaromi, I.; Martin, R. L.; Fox, D. J.; Keith, T.; Al-Laham, M. A.; Peng, C. Y.; Nanayakkara, A.; Challacombe, M.; Gill, P. M. W.; Johnson, B.; Chen, W.; Wong, M. W.; Gonzalez, C.; Pople, J. A.*Gaussian 03, Revision C.02*; Gaussian, Inc., Wallingford, CT, **2004**.

(18) (a) Perdew, J. P.; Burke, K.; Ernzerhof, M. *Phys. Rev. Lett.* **1996**, *77*, 3865. (b) Perdew, J. P.; Burke, K.; Ernzerhof, M. *Phys. Rev. Lett.* **1997**, *78*, 1396. (c) Perdew, J. P.; Burke, K.; Ernzerhof, M. *J. Chem. Phys.* **1996**, *105*, 9982. (d) Ernzerhof, M.; Scuseria, G. E. *J. Chem. Phys.* **1999**, *110*, 5029.

(19) (a) Schäfer, A.; Huber, C.; Ahlrichs, R. *J. Chem. Phys.* **1994**, *100*, 5829. (b) Eichkorn, K.; Weigend, F.; Treutler, O.; Ahlrichs, R. *Theor. Chem. Acc.* **1997**, *97*, 119.

(20) (a) Laaksonen, L. *J. Mol. Graph.* **1992**, *33*, 10. (b) Bergman, D. L.; Laaksonen, L.; Laaksonen, A. *J. Mol. Graph. Model.* **1997**, *15*, 301.

Synthesis of TMEDA·Li[HC(PPh$_2$Se)(PPh$_2$)] (Li7a). A mixture of TMEDA·Li[HC(PPh$_2$)$_2$] (0.507 g, 1.00 mmol) and elemental selenium (0.079 g, 1.00 mmol) in 30 mL of toluene was stirred for 10 min at −80 °C and 2^1/$_2$ h at 23 °C. The solvent was evaporated under vacuum, and the resulting oily product was treated with 10 mL of Et$_2$O, affording Li**7a** as a yellow powder (0.556 g, 95%). Anal. Calcd for $C_{31}H_{37}LiN_2P_2Se$: C, 63.59; H, 6.37; N, 4.78. Found: C, 63.38; H, 6.34; N, 4.58. ^{1}H NMR (d_8-THF, 23 °C): δ 6.83−7.66 (m, 20H, C_6H_5), 2.06 (s, 4H, −CH_2 of TMEDA), 1.90 (s, 12H, −CH_3 of TMEDA), 1.44 (dd, 1H, −CH of the PCP carbon, $^2J(^1H,^{31}P) = 7.6$ and 12.4 Hz). ^{13}C NMR (23 °C): δ 147.5 (dd, Ph, C_{ipso}, $^1J(^{13}C,^{31}P) = 10.6$ Hz, $^3J(^{13}C,^{31}P) = 1.6$ Hz), 144.6 (dd, Ph, C_{ipso}, $^1J(^{13}C,^{31}P) = 74.7$ Hz, $^3J(^{13}C,^{31}P) = 3.5$ Hz), 132.4 (d, Ph, C_{ortho}, $^2J(^{13}C,^{31}P) = 16.5$ Hz), 132.2 (d, Ph, C_{ortho}, $^2J(^{13}C,^{31}P) = 10.2$ Hz), 129.0 (d, Ph, C_{para}, $^4J(^{13}C,^{31}P) = 2.8$ Hz), 127.9 (d, Ph, C_{meta}, $^3J(^{13}C,^{31}P) = 6.6$ Hz), 127.5 (d, Ph, C_{meta}, $^3J(^{13}C,^{31}P) = 11.6$ Hz), 126.7 (s, Ph, C_{para}), 58.7 (s, TMEDA, −CH_2), 46.1 (s, TMEDA, −CH_3), 20.1 (dd, PCP carbon, $^1J(^{13}C,^{31}P) = 107.7$ Hz, $^1J(^{13}C,^{31}P) = 20.4$ Hz). ^{7}Li NMR (23 °C): δ 1.41. ^{31}P NMR (23 °C): δ 33.2 (d, $^2J(^{31}P,^{31}P) =$ 173.7 Hz, $^1J(^{31}P,^{77}Se) = 556$ Hz,), −10.9 (d, br, $^2J(^{31}P,^{31}P) =$ 173.7 Hz). ^{77}Se NMR (23 °C): δ −203 (dd, $^1J(^{77}Se,^{31}P) = 557$ Hz, $^2J(^{77}Se,^{31}P) = 12.6$ Hz). X-ray-quality crystals of Li**7a** were obtained by dissolving the yellow powder in boiling toluene and then cooling the solution to room temperature in ca. 10 h.

Synthesis of TMEDA·Li[HC(PPh$_2$Te)(PPh$_2$)] (Li7b). A mixture of TMEDA·Li[HC(PPh$_2$)$_2$] (0.253 g, 0.50 mmol) and elemental tellurium (0.064 g, 0.50 mmol) in 40 mL of toluene was stirred for 10 min at −80 °C and 2^1/$_2$ h at 23 °C. A small amount of unreacted tellurium was removed by filtration, and the solvent was evaporated under vacuum. Washing with *n*-hexane afforded Li**7b** as a bright yellow powder (0.260 g, 82%, calculated as Li**7b**) in ca. 97% purity; removal of the spectroscopically detectable byproduct [H$_2$C(PPh$_2$)$_2$] and TMEDA·Li[HC(PPh$_2$Te)$_2$] (Li**8b**) was not possible due to the extreme moisture sensitivity of Li**7b**. ^{1}H NMR (d_8-THF, 23 °C): δ 7.12−7.92 (m, 20H, C_6H_5), 2.34 (s, 4H, −CH_2 of TMEDA), 2.17 (s, 12H, −CH_3 of TMEDA), 1.61 (s, br, 1H, −CH of the PCP carbon). ^{13}C NMR (23 °C): δ 148.3 (s, br Ph, C_{ipso}), 144.2 (s, br, Ph, C_{ipso}), 132.9 (s, br, Ph, C_{ortho}), 128.9 (s, br, Ph, C_{para}), 127.3 (s, br, Ph, C_{meta}), 126.5 (s, br, Ph, C_{para}), 58.7 (s, TMEDA, −CH_2), 46.2 (s, TMEDA, −CH_3), 22.0 (s, br, PCP carbon). ^{7}Li NMR (23 °C): δ 1.01. ^{31}P NMR (23 °C): δ −4.4 (d, $^2J(^{31}P,^{31}P) =$ 181.9 Hz), −14.2 (d, $^2J(^{31}P,^{31}P) = 181.9$ Hz, $^1J(^{31}P,^{125}Te) = 1359$ Hz). ^{125}Te NMR (23 °C): δ −374 (d, br, $^1J(^{125}Te,^{31}P) = 1358$ Hz). X-ray-quality crystals of Li**7b** were obtained by dissolving the yellow powder in boiling *n*-hexane and then cooling the solution to room temperature in ca. 2 h.

Synthesis of TMEDA·Li[HC(PPh$_2$Se)$_2$] (Li8a). A mixture of TMEDA·Li[HC(PPh$_2$)$_2$] (0.507 g, 1.00 mmol) and elemental selenium (0.166 g, 2.10 mmol, slight excess) in 50 mL of toluene was stirred for 10 min at −80 °C, 1$/$$_2$ h at 23 °C, and 2^1/$_2$ h at 55 °C. The excess selenium was removed by filtration, and the solvent was evaporated under vacuum. The resulting amorphous product was washed with 20 mL of *n*-hexane, affording Li**8a** as a pale yellow powder (0.618 g, 93%). Anal. Calcd for $C_{31}H_{37}LiN_2P_2Se_2$: C, 56.04; H, 5.61; N, 4.22. Found: C, 55.73; H, 5.54; N, 4.05. ^{1}H NMR (d_8-THF, 23 °C): δ 7.25−8.01 (m, 20H, C_6H_5), 2.32 (s, 4H, −CH_2 of TMEDA), 2.14 (s, 12H, −CH_3 of TMEDA), 1.54 (t, 1H, −CH of the PCP carbon, $^2J(^1H,^{31}P) = 2.2$ Hz). ^{13}C NMR (23 °C): δ 141.5 (dd, Ph, C_{ipso}, $^1J(^{13}C,^{31}P) = 90.7$ Hz, $^3J(^{13}C,^{31}P) = 6.6$ Hz), 132.6 (m, Ph, C_{ortho}, $^2J(^{13}C,^{31}P) = 5.5$ Hz), 129.7 (s, Ph, C_{para}), 127.8 (m, Ph, C_{meta}, $^3J(^{13}C,^{31}P) = 6.0$ Hz), 58.5 (s, TMEDA, −CH_2), 46.2 (s, TMEDA, −CH_3), 18.4 (t, PCP carbon, $^1J(^{13}C,^{31}P) = 100.4$ Hz). ^{7}Li NMR (23 °C): δ 1.20. ^{31}P NMR (23 °C): δ 25.1 (s, $^1J(^{31}P,^{77}Se) = 585$ Hz, $^2J(^{31}P,^{31}P) = 30.1$ Hz). ^{77}Se NMR (23 °C): δ −166.2 (d, $^1J(^{77}Se,^{31}P) = 585$ Hz). X-ray-quality crystals of Li**8a** were obtained by dissolving the yellow powder in boiling toluene and then cooling the solution to room temperature in ca. 3 h.

Attempted Synthesis of TMEDA·Li[HC(PPh$_2$Te)$_2$] (Li8b). A mixture of TMEDA·Li[HC(PPh$_2$)$_2$] (0.253 g, 0.50 mmol) and elemental tellurium (0.128 g, 1.00 mmol) in 40 mL of toluene was stirred for 10 min at −80 °C and 24 h at 23 °C. After 3 h the ^{31}P NMR spectrum showed a ca. 2:1:1 mixture of TMEDA·Li[HC(PPh$_2$Te)(PPh$_2$)] (Li**7b**), [H$_2$C(PPh$_2$)$_2$], and TMEDA·Li[HC(PPh$_2$Te)$_2$] (Li**8b**). Increased reaction time (up to 24 h) and/or elevated temperature resulted in decomposition and, eventually, the formation of [H$_2$C(PPh$_2$)$_2$] as the sole product containing the PCP unit (^{31}P NMR). NMR data for TMEDA·Li[HC(PPh$_2$Te)$_2$] (Li**8b**): ^{31}P NMR (d_8-THF, 23 °C): δ −27.0 (s, $^1J(^{31}P,^{125}Te) = 1376$ Hz, $^2J(^{31}P,^{31}P) = 40.3$ Hz); ^{125}Te NMR (23 °C): δ −245 (d, br, $^1J(^{125}Te,^{31}P) = 1380$ Hz).

Synthesis of TMEDA·Li[HC(P^{i}Pr$_2$Se)$_2$] (Li8c). A solution of [H$_2$C(PCl$_2$)$_2$] (0.871 g, 4.00 mmol) in 40 mL of THF was cooled to −80 °C, and a solution of ^{i}PrMgCl (8.0 mL of 2.0 M solution in THF) was added via syringe. The reaction mixture was stirred for 10 min at −80 °C, 1$/$$_2$ h at 23 °C, and 3 h at 50 °C. Solvent was evaporated under vacuum, and the oily product, [H$_2$C(P^{i}Pr$_2$)$_2$], was extracted with ca. 100 mL of Et$_2$O. After filtration through a PTFE disk (to remove MgCl$_2$), the solvent was evaporated and the product was dissolved in 40 mL of THF (^{31}P NMR of [H$_2$C(P^{i}Pr$_2$)$_2$] δ −1.3 in THF; cf. lit.[21] value of 1.3 ppm in CDCl$_3$). This solution was added to a flask containing 0.632 g of elemental selenium (8.00 mmol), and the reaction mixture was stirred for 5 h at 23 °C. The full conversion of both P(III) centers to P(V) in [H$_2$C(P^{i}Pr$_2$Se)$_2$] was confirmed by ^{31}P NMR spectroscopy (δ 56.8, $^1J(^{31}P,^{77}Se) = 726$ Hz and $^2J(^{31}P,^{31}P) = 17.0$ Hz in THF).

A solution of LiN^{i}Pr$_2$ (0.450 g, 4.20 mmol, 5% excess) in 20 mL of THF was added to the solution of [H$_2$C(P^{i}Pr$_2$Se)$_2$] at 23 °C. The reaction mixture was stirred for 1$/$$_2$ h, and then a solution of TMEDA (0.488 g, 4.20 mmol, 5% excess) was added via cannula and stirring was continued for an additional 3 h. The solvent was evaporated under vacuum, and the product was dissolved in 70 mL of toluene followed by filtration to remove the remaining LiN^{i}Pr$_2$. Solvent removal gave a sticky product, which was washed with pentane to give Li**8c** as a pale yellow powder (1.776 g, 84%). Anal. Calcd for $C_{19}H_{45}LiN_2P_2Se_2$: C, 43.19; H, 8.58; N, 5.30. Found: C, 42.81; H, 8.31; N, 5.36. ^{1}H NMR (d_8-THF, 23 °C): δ 2.67 (s, 4H, −CH_2 of TMEDA), 2.53 (s, 12H, −CH_3 of TMEDA), 2.27 (m, 4H, −CH of ^{i}Pr), 1.47 (m, 24H, −CH_3 of ^{i}Pr), 0.59 (s, 1H, −CH of the PCP carbon). ^{13}C NMR (23 °C): δ 58.4 (s, TMEDA, −CH_2), 46.3 (s, TMEDA, −CH_3), 32.33 (d, ^{i}Pr, −CH, $^1J(^{13}C,^{31}P) = 55.0$ Hz), 17.8 (d, ^{i}Pr, −CH_3, $^2J(^{13}C,^{31}P) = 4.1$ Hz), 4.0 (t, PCP carbon, $^1J(^{13}C,^{31}P) =$ 97.5 Hz). ^{7}Li NMR (23 °C): δ 1.05. ^{31}P NMR (23 °C): δ 52.5 (s, $^1J(^{31}P,^{77}Se) = 563$ Hz, $^2J(^{31}P,^{31}P) = 13.1$ Hz). ^{77}Se NMR (23 °C): δ −355.2 (d, $^1J(^{77}Se,^{31}P) = 563$ Hz). X-ray-quality crystals of Li**8c** were obtained from Et$_2$O solution at 5 °C in 12 h.

Synthesis of {Zn[HC(PPh$_2$Se)$_2$]$_2$} (9a). A solution of ZnCl$_2$ (0.034 g, 0.25 mmol) in 15 mL of THF was cooled to −80 °C, and a solution of TMEDA·Li[HC(PPh$_2$Se)$_2$] (Li**8a**; 0.332 g, 0.50 mmol) in 20 mL of THF was added via cannula. The reaction mixture was stirred for 1$/$$_2$ h at −80 °C and 2 h at 23 °C. The solvent was evaporated under vacuum, and the product was washed with cold Et$_2$O (0 °C) to remove H$_2$C(PPh$_2$Se)$_2$ byproduct and then dissolved in toluene. TMEDA·LiCl was filtered from the toluene solution followed by solvent evaporation to afford **9a** as a pale yellow powder (0.138 g, 48%). Anal. Calcd for $C_{50}H_{42}P_4Se_4Zn$: C, 52.31; H, 3.69. Found: C, 52.42; H, 3.83. ^{1}H NMR (d_8-THF, 23 °C): δ 7.26−7.87 (m, 20H, C_6H_5), 1.72 (s, 1H, −CH of the PCP carbon). ^{13}C NMR (23 °C): δ 137.0 (d, Ph,

(21) Wolf, J.; Manger, M.; Schmidt, U.; Fries, G.; Barth, D.; Weberndörfer, B.; Vicic, D. A.; Jones, W. D.; Werner, H. *J. Chem. Soc., Dalton Trans.* **1999**, 1867.

C_{ipso}, $^1J(^{13}C,^{31}P) = 89.9$ Hz), 132.7 (m, Ph, C_{ortho}, $^2J(^{13}C,^{31}P) = 5.5$ Hz), 131.1 (s, Ph, C_{para}), 128.5 (m, Ph, C_{meta}, $^3J(^{13}C,^{31}P) = 6.5$ Hz), 15.5 (t, PCP carbon, $^1J(^{13}C,^{31}P) = 88.0$ Hz). ^{31}P NMR (23 °C): δ 25.4 (s, $^1J(^{31}P,^{77}Se) = 502$ Hz, $^2J(^{31}P,^{31}P) = 22.3$ Hz). ^{77}Se NMR (23 °C): δ −124.2 (d, $^1J(^{77}Se,^{31}P)$ 501 Hz). X-ray-quality crystals were obtained by layering *n*-hexane on top of the toluene solution of **9a** after 24 h at +5 °C.

Synthesis of {Hg[HC(PPh$_2$Se)$_2$]$_2$} (9b). A solution of $HgCl_2$ (0.081 g, 0.30 mmol) in 15 mL of THF was cooled to −80 °C, and a solution of TMEDA·Li[HC(PPh$_2$Se)$_2$] (Li**8a**; 0.399 g, 0.60 mmol) in 20 mL of THF was added via cannula. The reaction mixture was stirred for $^1/_2$ h at −80 °C and 2 h at 23 °C. The solvent was evaporated under vacuum, and the product was dissolved in toluene. TMEDA·LiCl was removed by filtration followed by solvent removal to afford **9b** as a pale yellow powder (0.298 g, 77%). Anal. Calcd for $C_{50}H_{42}P_4Se_4Hg$: C, 46.80; H, 3.30. Found: C, 47.10; H, 3.49. ^{1}H NMR (d_8-THF, 23 °C): δ 7.30−7.86 (m, 20H, C_6H_5), 1.76 (s, 1H, −C*H* of the PCP carbon). ^{13}C NMR (23 °C): δ 137.4 (d, Ph, C_{ipso}, $^1J(^{13}C,^{31}P) = 89.8$ Hz), 132.7 (m, Ph, C_{ortho}, $^2J(^{13}C,^{31}P) = 5.6$ Hz), 131.2 (s, Ph, C_{para}), 128.6 (m, Ph, C_{meta}, $^3J(^{13}C,^{31}P) = 6.3$ Hz), 16.1 (t, PCP carbon, $^1J(^{13}C,^{31}P) = 89.6$ Hz). ^{31}P NMR (23 °C): δ 26.0 (s, $^1J(^{31}P,^{77}Se) = 510$ Hz, $^2J(^{31}P,^{31}P) = 20.5$ Hz, $^2J(^{31}P,^{199}Hg) = 109.2$ Hz). ^{77}Se NMR (23 °C): δ −82.3 (d, $^1J(^{77}Se,^{31}P)$ 510 Hz). ^{199}Hg NMR (23 °C): δ −793.2 (s, br). X-ray-quality crystals were obtained by layering Et_2O on top of a THF solution of **9b** for 4 h at +5 °C.

Oxidation of TMEDA·Li[HC(PPh$_2$Se)$_2$] (Li8a) and TMEDA·Li[HC(P^{i}Pr$_2$Se)$_2$] (Li8c) with I$_2$. A solution of TMEDA·Li[HC(PPh$_2$Se)$_2$] (Li**8a**; 0.066 g, 0.10 mmol) in 30 mL of THF was cooled to −80 °C, and a solution of I_2 (0.013 g, 0.05 mmol) in 30 mL of THF was added via cannula. The reaction mixture was warmed to ca. −50 °C, at which point the red solution became bright red (cherry). This solution was used for EPR spectroscopic measurements. The remaining reaction solution was allowed to reach room temperature, which resulted in the disappearance of the red color to give a pale yellow solution. NMR spectroscopy revealed the formation of [H$_2$C(PPh$_2$Se)$_2$]: ^{1}H NMR (d_8-toluene, 23 °C) δ 6.92−7.87 (m, 20H, C_6H_5), 4.20 (t, 2H, −C*H* of the PCP carbon, $^2J(^1H,^{31}P) = 13.2$ Hz); ^{31}P NMR (23 °C): δ 26.3 (s, $^1J(^{31}P,^{77}Se) = 763$ Hz, $^2J(^{31}P,^{31}P) = 18.6$ Hz).[22]

The one-electron oxidation of TMEDA·Li[HC(P^{i}Pr$_2$Se)$_2$] (Li**8c**) was performed similarly as described above for Li**8a** by using 0.106 g of Li**8c** (0.20 mmol) and 0.025 g of I_2 (0.10 mmol) in 70 mL of THF. In this case, however, only a steady darkening of the initial red color of the solution was observed when the reaction mixture slowly warmed up. Similarly to Li**8a**, the ^{31}P NMR spectrum of the reaction solution showed the neutral [H$_2$C(P^{i}Pr$_2$Se)$_2$] as the sole product after 1 h at 23 °C (δ 56.8 with $^1J(^{31}P,^{77}Se) = 726$ Hz and $^2J(^{31}P,^{31}P) = 17.0$ Hz in THF). Samples for EPR spectroscopy were taken at −80 °C and at −50 °C, and the spectra were run in the temperature range −70 to +20 °C.

Results and Discussion

Synthesis and Spectroscopic Characterization of TMEDA·Li[HC(PPh$_2$E)(PPh$_2$)] (E = Se (Li7a), Te (Li7b)) and TMEDA·Li[HC(PPh$_2$E)$_2$)] (E = Se (Li8a), Te (Li8b)). The synthesis of the monoanions **7** and **8** entails two major challenges that, in part, may provide an explanation for the lack of information for these compounds in the literature. First, similar to the behavior of [HN(PPh$_2$)$_2$],[4] elemental tellurium *does not* react with the neutral bis(diphenylphosphinoyl)methane, [H$_2$C(PPh$_2$)$_2$]. Second, a limited spectroscopic study of the monochalcogeno anions **7** showed that, in contrast to the analogous sulfur compounds, organolithium reagents (RLi) react with the P−Se functionality in [H$_2$C(PPh$_2$Se)(PPh$_2$)] with the subsequent formation of RSeLi and/or R_2Se.[23] Consequently, we adopted the synthetic strategy that was successful for the production of the related tellurium-containing anion $[N(PR_2Te)_2]^-$ (**1**).[4] In this procedure the anion $[HC(PR_2)_2]^-$[14] is generated *prior to* oxidation of the phosphorus(III) center(s) with elemental chalcogen(s) (Scheme 1).

Scheme 1. Formation of the Monoanions **7** and **8**

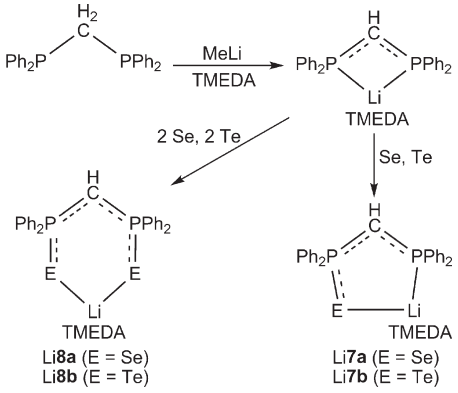

The reactions of TMEDA·Li[HC(PPh$_2$)$_2$] with 1 equiv of elemental selenium or tellurium in toluene at room temperature to produce Li**7a** and Li**7b**, respectively, are complete after $2^1/_2$ h. The ^{31}P NMR spectra of these lithium derivatives (d_8-THF, 23 °C) show the expected inequivalence of the P(III) and P(V) centers in the form of two mutually coupled doublets at 33.2 and −10.9 ppm (Li**7a**) and at −4.4 and −14.2 ppm (Li**7b**). The $^2J(^{31}P,^{31}P)$ coupling constants show unusually high values of ca. 175−180 Hz: cf. 50−85 Hz in the neutral $P^{III}CH_2P^V$ systems [H$_2$C(PPh$_2$E)(PPh$_2$)] (E = O, S, Se).[22] In these asymmetric, neutral compounds the large coupling constants have been attributed to a combination of increased s character in the phosphorus bonds and to a change in the difference of effective nuclear charge between the phosphorus atoms.[24] The larger coupling constants in the anions **7** therefore suggest even greater charge difference between the phosphorus centers than in the analogous neutral systems. The ^{77}Se and ^{125}Te satellites are observable in the ^{31}P NMR resonances at 33.2 (Li**7a**) and −14.2 ppm (Li**7b**). The magnitude of the coupling constants of $^1J(^{31}P,^{77}Se) = 556$ Hz and $^1J(^{31}P,^{125}Te) = 1359$ Hz is significantly smaller than the values of ca. 760 and 1650 Hz typically observed for terminal P=Se and P=Te bonds, respectively, thus suggesting a considerable Li−E interaction (E = Se, Te) and formation of a five-membered ring in Li**7a** and Li**7b**, as illustrated in Scheme 1 (cf. for example $^1J(^{31}P,^{77}Se) = 763$ Hz in [H$_2$C(PPh$_2$Se)$_2$][22] and $^1J(^{31}P,^{125}Te) = 1654$ Hz in [N(P^{i}Pr$_2$Te)(P^{i}Pr$_2$H)][5]). Furthermore, the two notably different $^1J(^{13}C,^{31}P)$ coupling constants of 108 and 20 Hz obtained for the PCP carbon from the ^{13}C NMR spectrum of Li**7a** indicates a

(22) Grim, S. O.; Walton, E. D. *Inorg. Chem.* **1980**, *19*, 1982.

(23) Lusser, M.; Peringer, P. *Inorg. Chim. Acta* **1987**, *127*, 151.

(24) (a) Grim, S. O.; Mitchell, J. D. *Inorg. Chem.* **1977**, *16*, 1762. (b) Keiter, R. L.; Cary, L. W. *J. Am. Chem. Soc.* **1972**, *94*, 9232. (c) Bertrand, R. D.; Allison, D. A.; Verkade, J. G. *J. Am. Chem. Soc.* **1970**, *92*, 71. (d) Bertrand, R. D.; Ogilvie, F. B.; Verkade, J. G. *J. Am. Chem. Soc.* **1970**, *92*, 1908.

substantial inequality in the P−C bond lengths. Interestingly, the selenium-bound ^{31}P(Se) chemical shift in Li**7a** is markedly downfield from the value of −3.7 ppm observed for the anion $[HC(PPh_2)_2]^-$,[25] whereas the ^{31}P(Te) signal in Li**7b** exhibits a high-field shift compared to the starting material.

While the monoseleno anion Li**7a** is isolated as a relatively stable compound, the tellurium analogue Li**7b** exhibits thermal instability; the yellow powder starts to darken in a few minutes even in an inert atmosphere glovebox (with oxygen levels less than 3 ppm) at room temperature. In addition, the ^{31}P NMR spectrum of the reaction solution of Li**7b** after $2^1/_2$ h shows two minor signals (ca. 3%) attributed to $[H_2C(PPh_2)_2]$ (δ −21.4) and TMEDA·Li$[HC(PPh_2Te)_2]$ (Li**8b**, δ −27.0; vide infra); after prolonged standing only the former byproduct is observed in the ^{31}P NMR spectrum. A similar disproportionation of the related P^{III}/P^V system Li$[N(P^iPr_2Te)(P^iPr_2)]$ to give the symmetrical P^{III}/P^{III} and P^V/P^V compounds $[HN(P^iPr_2)_2]$ and Li$[N(P^iPr_2Te)_2]$, respectively, has been previously reported.[3] This disproportionation, presumably, also contributes to the broadness of the signals in the NMR spectra of Li**7b**. The $^1J(^{13}C,^{31}P)$ coupling constants could not be obtained from the ^{13}C NMR spectrum, and only a very broad doublet is observed in the ^{125}Te NMR spectrum, whereas the ^{77}Se NMR spectrum of Li**7a** displays a well-resolved doublet of doublets due to the $^1J(^{77}Se,^{31}P)$ and $^2J(^{77}Se,^{31}P)$ couplings.

The oxidation of TMEDA·Li$[HC(PPh_2)_2]$ with 2 equiv of elemental selenium in toluene requires moderate heating (55 °C) to complete the formation of Li**8a** (Scheme 1). The ^{31}P NMR spectrum of Li**8a** (d_8-THF, 23 °C) exhibits a singlet at 25.1 ppm with ^{77}Se satellites showing $^1J(^{77}Se,^{31}P)$ and $^2J(^{31}P,^{31}P)$ coupling constants of 585 and 30.1 Hz, respectively. The latter value is considerably smaller than that observed for Li**7a**, indicative of the change in the difference of effective nuclear charge between the two phosphorus centers:[24] i.e., the Li−P contact in the asymmetric Li**7a** has likely been replaced by a P−Se bond in Li**8a**. The ^{77}Se NMR spectrum of Li**8a** exhibits a doublet at −166 ppm, ca. 35 ppm downfield from the signal observed for Li**7a**, and the $^1J(^{13}C,^{31}P)$ coupling constant of 100 Hz, obtained from the PCP carbon resonance at 18.4 ppm in the ^{13}C NMR spectrum of Li**8a**, is close to one of the two inequivalent couplings resolved for Li**7a**. Taken together, these NMR data suggest formation of the expected LiSePCPSe six-membered ring with equivalent P(V) atoms for Li**8a**.

The reaction between elemental tellurium and TMEDA·Li$[HC(PPh_2)_2]$ in a 2:1 molar ratio is more complicated than the corresponding reaction with selenium. After 3 h at 23 °C the ^{31}P NMR spectrum of the reaction mixture shows resonances attributed to Li**7b** (doublets at −4.4 and −14.2 ppm) and $[H_2C(PPh_2)_2]$ (δ −21.4), in addition to a singlet at −27.0 ppm. The last signal exhibits ^{125}Te satellites with the $^1J(^{31}P,^{125}Te)$ and $^2J(^{31}P,^{31}P)$ coupling constants of 1376 and 40.3 Hz, respectively. The former coupling is somewhat bigger than that obtained for the asymmetric monotelluro compound Li**7b**, and the latter coupling is in the same range as that observed for the diseleno anion in Li**8a**. In addition, a broad doublet is resolved in the ^{125}Te NMR spectrum of the reaction mixture at −245 ppm, ca. 130 ppm downfield from that of Li**7b**, with a $^1J(^{31}P,^{125}Te)$ coupling constant of 1380 Hz. Comparison of these NMR data with those of the monotelluro compound Li**7b** and the selenium congeners Li**7a** and Li**8a** is consistent with the formation of ditelluro anion in Li**8b**. However, longer reaction times or even moderate heating leads to decomposition to yield neutral $[H_2C(PPh_2)_2]$; consequently, we have not been able to isolate a pure sample of Li**8b**.

Synthesis and Spectroscopic Characterization of TMEDA·Li$[HC(P^iPr_2Se)_2]$ (Li8c). While the parent PCP backbone in **7** and **8** as the phenyl derivative, $[H_2C(PPh_2)_2]$, is easily available from commercial sources, the preparation of other (especially alkyl) derivatives is hampered by multistep and/or low-yield processes.[26] However, by using commercially available bis(dichlorophosphinoyl)methane, $[H_2C(PCl_2)_2]$, in a reaction with 4 equiv of the Grignard reagent ^{i}PrMgCl, the isopropyl derivative is readily obtained in quantitative yield (>95%; eq 1). The purity of this colorless oil was confirmed by ^{31}P NMR spectroscopy[21] prior to in situ reaction with 2 equiv of elemental selenium (eq 2) followed by (in situ) deprotonation with LiN^iPr_2 in the presence of TMEDA (eq 3). This three-step process affords analytically pure TMEDA·Li$[HC(P^iPr_2Se)_2]$ (Li**8c**) in excellent yield (84%, calculated from $[H_2C(PCl_2)_2]$).

$$[H_2C(PCl_2)_2] + 4^iPrMgCl \rightarrow [H_2C(P^iPr_2)_2] + 4MgCl_2 \quad (1)$$

$$[H_2C(P^iPr_2)_2] + 2Se \rightarrow [H_2C(P^iPr_2Se)_2] \quad (2)$$

$$[H_2C(P^iPr_2Se)_2] + LiN^iPr_2 + TMEDA \rightarrow TMEDA\cdot Li[HC(P^iPr_2Se)_2] + HN^iPr_2$$

Li**8c** (3)

The ^{31}P NMR spectrum of Li**8c** shows a singlet at 52.5 ppm with $^1J(^{31}P,^{77}Se)$ of 563 Hz and $^2J(^{31}P,^{31}P)$ of 13.1 Hz, indicative of only a slight change in the P−Se bond length compared to the phenyl derivative Li**8a**. The triplet resolved at 4.0 ppm for the PCP carbon in the ^{13}C NMR spectrum of Li**8c** exhibits a $^1J(^{13}C,^{31}P)$ coupling constant of 97.5 Hz (cf. 100.4 Hz in Li**8a**), and a singlet is observed at 0.59 ppm for the corresponding hydrogen in the ^{1}H NMR spectrum. In both of these spectra the typical signal patterns are also seen for the ^{i}Pr and TMEDA groups. In addition, a doublet is found at −355.2 ppm in the ^{77}Se NMR spectrum of Li**8c** with a $^1J(^{77}Se,^{31}P)$ value of 563 Hz, which is ca. 160 Hz smaller than that in the neutral precursor, $[H_2C(P^iPr_2Se)_2]$ (see the Experimental Section), thus indicating the expected coordination of the lithium atom to two selenium centers.

(25) Colquhoun, I. J.; McFarlane, C. E.; McFarlane, W. *J. Chem. Soc., Chem. Commun.* **1982**, 220.

(26) For a large-scale, multistep synthesis of a variety of derivatives $[H_2C(PR_2)(PR'_2)]$, see:Eisenträger, F.; Göthlich, A.; Gruber, I.; Heiss, H.; Kiener, C. A.; Kruger, C.; Notheis, J. U.; Rominger, F.; Scherhag, G.; Schultz, M.; Straub, B. F.; Volland, M. A. O.; Hofmann, P. *New J. Chem.* **2003**, *27*, 540.

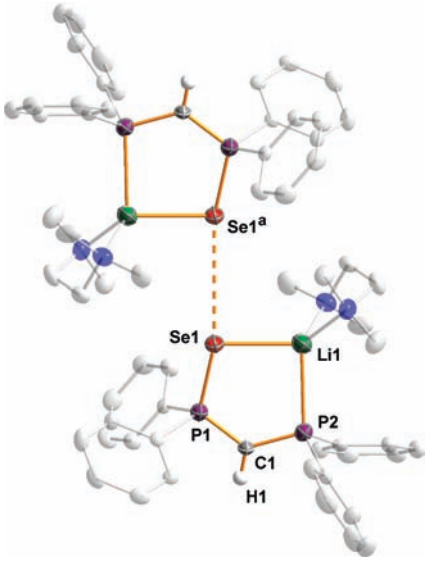

Figure 1. Crystal structure of TMEDA·Li[HC(PPh$_2$Se)(PPh$_2$)] (Li**7a**) with thermal ellipsoids at the 50% probability level. Hydrogen atoms in the phenyl groups and in TMEDA have been omitted for clarity. The tellurium analogue Li**7b** is isostructural with Li**7a**. Symmetry operation: (a) $-x$, $1-y$, $-z$ (Li**7a**) and $1-x$, $1-y$, $1-z$ (Li**7b**).

Crystal Structures of TMEDA·Li[HC(PPh$_2$E)(PPh$_2$)] (E = Se (Li7a), Te (Li7b)) and TMEDA·Li[HC(PR$_2$Se)$_2$] (R = Ph (Li8a), ^{i}Pr (Li8c)). The X-ray structural determinations of Li**7a** and Li**7b** confirm the formation of the five-membered ELiPCP ring (E = Se, Te) inferred from the NMR data (Figure 1). In the crystal lattice both structures appear as centrosymmetric dimers created by an intermolecular E···E close contact that is somewhat stronger for the tellurium compound Li**7b** (3.514(1) Å (Li**7b**) vs 3.6407(6) Å (Li**7a**); Table 2) (cf. sums of the van der Waals radii for Se and Te at 4.00 and 4.40 Å, respectively).[27] Presumably the steric strain between TMEDA and phenyl units is reduced in Li**7b** compared to Li**7a** as a result of the longer Te−P and Te−Li bonds. The five-membered ring in Li**7a** and Li**7b** displays a moderate distortion from planarity, with the dihedral angles spanning a range of 1−19°. The change of chalcogens between Li**7a** and Li**7b** results in a difference of ca. 4° in the bond angles at the E1 (E = Se, Te) and P2 atoms, while the remaining bond angles are approximately equal.

As indicated by the calculated bond orders (Table 2),[28] the Li−E contact in both Li**7a** and Li**7b** (E = Se, Te) approaches a covalent bond with a value of 0.9, whereas the Li−P bond is somewhat weaker with a bond order of 0.5. Furthermore, consistent with the two inequivalent $^1J(^{13}C,^{31}P)$ coupling constants resolved for the PCP carbon in Li**7a**, the P−C bond lengths in both Li**7a** and Li**7b** show a disparity of ca. 0.04 Å, the shorter bond involving the chalcogen-bound phosphorus(V) atom. These data are indicative of substantial contribution from a resonance structure in which the phosphorus(III) center

Scheme 2. Major Resonance Form in Li**7a** and in the Analogous Monotelluroimidodiphosphinates

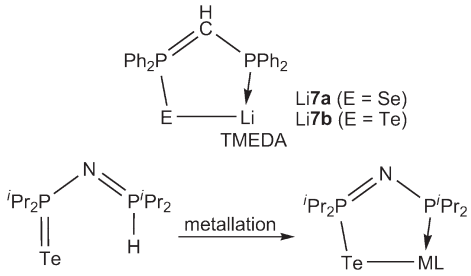

forms a dative bond with lithium and the phosphorus(V) atom is connected to the PCP carbon with a double bond (Scheme 2). A similar bonding arrangement has been suggested in monotelluroimidodiphosphinate monoanions **1** after metalation of the P−H unit in the neutral [N(P^iPr_2Te)(P^iPr_2H)] (Scheme 2).[3]

The crystal structures of Li**8a** and Li**8c** are illustrated in Figure 2, and the pertinent bond parameters are summarized in Table 3. The structures of Li**8a** and Li**8c** corroborate the formation of the expected six-membered ring with two P−Se bonds and Li−Se contacts (Scheme 1). The P−Se and Li−Se bond lengths in the structure of the diseleno derivative Li**8a** are analogous to those seen in the monoseleno analogue Li**7a**, while the P−C distances are intermediate between the two values observed in the PCP unit for Li**7a**. The change of substituents on phosphorus atoms in Li**8c** has virtually no effect on the bond lengths compared to Li**8a**. The dihedral angles reveal a slightly more puckered six-membered ring in Li**8a** than in the isopropyl derivative Li**8c**, and the P−C−P angle shows a widening of ca. 6° for the latter compound. The bond angles at selenium atoms are also somewhat wider in Li**8c**, while the angles at the phosphorus centers in Li**8a** and Li**8c** are equal.

Synthesis and Characterization of {M[HC(PPh$_2$Se)$_2$]$_2$} (M = Zn (9a); Hg (9b)). The monochalcogeno compounds Li**7a** and Li**7b** have been used as in situ reagents in metathetical reactions with $HgCl_2$ to generate homoleptic complexes, which were inferred to involve P,E chelation of the ligand to the metal center on the basis of solution NMR data.[23] Alkali-metal derivatives of diselenoimidodiphosphinate anions of the type **2** (E = Se) have been widely used in the synthesis of a variety of metal complexes of main-group and transition-metal elements,[1] which have subsequently been utilized as single-source precursors of metal selenides.[30] In this initial study of the dichalcogeno bis(phosphinoyl)methane anion **8**, the reactions between Li**8a** and MCl_2 (M = Zn, Hg) were conducted in a 2:1 molar ratio in order to establish the viability of the new reagent in metathesis with metal halides. The reaction with $HgCl_2$ in toluene at −80 °C proceeded cleanly to produce {Hg[HC(PPh$_2$Se)$_2$]$_2$} (**9b**) in good yield, whereas the synthesis of the zinc congener

(27) Pauling, L. *The Nature of the Chemical Bond*, 3rd ed.; Cornell University Press: Ithaca, NY, 1960.

(28) Bond orders were calculated by the Pauling equation $N = 10^{(D-R)/0.71}$,[27] where R is the observed bond length (Å). The single bond length D is estimated from the sums of appropriate covalent radii (Å): [27,29] Li−P, 2.35; Li−Se, 2.48; Li−Te, 2.66; Se−P, 2.27; Te−P, 2.45.

(29) Cordero, B.; Gomez, V.; Platero-Prats, A. E.; Reves, M.; Echeverria, J.; Cremades, E.; Barragan, F.; Alvarez, S. *Dalton Trans.* **2008**, 2832.

(30) For selected examples, see: (a) Afzaal, M.; Crouch, D.; Malik, M. A.; Motevalli, M.; O'Brien, P.; Park, J.-H. *J. Mater. Chem.* **2003**, *13*, 639. (b) Afzaal, M.; Ellwood, K.; Pickett, N. L.; O'Brien, P.; Raftery, J.; Waters, J. *J. Mater. Chem.* **2004**, *14*, 1310. (c) Waters, J.; Crouch, D. J.; Raftery, J.; O'Brien, P. *Chem. Mater.* **2004**, *16*, 3289. (d) Afzaal, M.; Crouch, D.; Malik, M. A.; Motevalli, M.; O'Brien, P.; Woollins, J. D. *Eur. J. Inorg. Chem.* **2004**, 171. (e) Crouch, D. J.; Hatton, P. M.; Helliwell, M.; O'Brien, P.; Raftery, J. *Dalton Trans.* **2003**, 2761.

Table 2. Selected Bond Lengths (Å) and Angles (deg) in Li**7a** and Li**7b**[a,28]

	Li**7a**[b]	Li**7b**[c]		Li**7a**[b]	Li**7b**[c]
E1−P1	2.1591(6) [1.43]	2.404(1) [1.16]	P1−C1	1.704(2)	1.693(4)
E1−Li1	2.510(3) [0.91]	2.700(6) [0.88]	P2−C1	1.739(2)	1.743(4)
Li1−P2	2.554(3) [0.52]	2.578(6) [0.48]	E1···E1′	3.6407(6)[d]	3.514(1)[e]
P1−E1−Li1	98.2(1)	94.1(1)	Li1−E1−P1−C1	12.0(1)	12.2(2)
C1−P1−E1	116.7(1)	115.9(1)	E1−P1−C1−P2	2.7(2)	0.9(3)
P2−C1−P1	123.2(1)	124.6(2)	P1−C1−P2−Li1	15.9(2)	14.8(3)
Li1−P2−C1	105.2(1)	109.5(2)	C1−P2−Li1−E1	18.9(1)	18.6(2)
E1−Li1−P2	92.5(1)	92.2(2)	P2−Li1−E1−P1	15.9(1)	14.9(2)

[a] Calculated bond orders are given in brackets. [b] E = Se. [c] E = Te. Symmetry operation for the atoms marked with a slanted prime (′). [d] $-x, 1-y, -z$. [e] $1-x, 1-y, 1-z$.

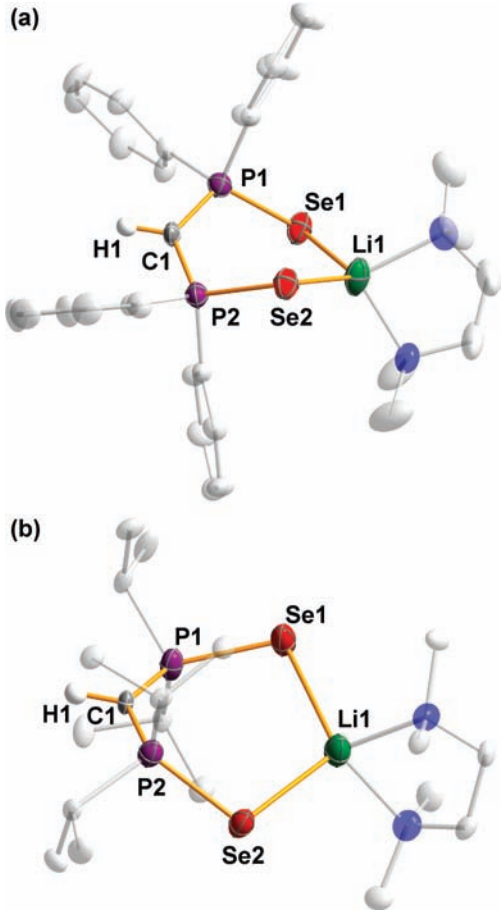

Figure 2. Molecular structure of (a) TMEDA·Li[HC($PPh_2Se)_2$] (Li**8a**) and (b) TMEDA·Li[HC($P^iPr_2Se)_2$] (Li**8c**) with thermal ellipsoids at the 50% probability level. Hydrogen atoms in the phenyl and isopropyl groups and in TMEDA have been omitted for clarity.

{Zn[HC($PPh_2Se)_2]_2$} (**9a**) afforded also a significant amount of the neutral [$H_2C(PPh_2Se)_2$] (^{31}P NMR) regardless of the reaction conditions or the source of $ZnCl_2$.

The ^{1}H NMR spectra of **9a** and **9b** show broad singlets at 1.72 and 1.76 ppm, respectively, for the hydrogen in the PCP unit, and triplets at 15.5 and 16.1 ppm with a $^1J(^{13}C,^{31}P)$ value of ca. 90 Hz is resolved for the corresponding carbon in the ^{13}C NMR spectra. The former resonances exhibit a high-field shift of ca. 1.2 ppm, and the latter signals are ca. 50 ppm to lower field with the $^1J(^{13}C,^{31}P)$ coupling constant ca. 45 Hz larger than the value observed for the only structurally characterized

Table 3. Selected Bond Lengths (Å) and Angles (deg) in Li**8a** and Li**8c**

	Li**8a**	Li**8c**		Li**8a**	Li**8c**
Se1−P1	2.144(2)	2.155(1)	Se2−Li1	2.59(1)	2.553(5)
Se1−Li1	2.54(1)	2.539(5)	P1−C1	1.720(6)	1.717(3)
Se2−P2	2.162(2)	2.158(1)	P2−C1	1.718(6)	1.717(3)
Li1−Se1−P1	98.7(2)	105.7(1)	Li1−Se1−P1−C1	56.8(4)	44.2(2)
Se1−P1−C1	118.0(2)	119.6(1)	Se1−P1−C1−P2	40.5(5)	−29.9(3)
P1−C1−P2	127.2(3)	133.6(2)	P1−C1−P2−Se2	36.3(6)	−25.3(3)
C1−P2−Se2	118.6(2)	119.5(1)	C1−P2−Se2−Li1	62.4(4)	45.7(2)
P2−Se2−Li1	94.7(2)	105.0(1)	P2−Se2−Li1−Se1	30.1(4)	−21.4(2)
Se2−Li1−Se1	113.6(4)	110.4(2)	Se2−Li1−Se1−P1	16.4(4)	−15.3(2)

complex of the [$HC(PPh_2Se)_2]^-$ anion, {Cp*Rh[HC-($PPh_2Se)_2$]ClO_4}.[13] Together with the absence of ^{199}Hg satellites for the PCP carbon resonance in the ^{13}C NMR spectrum of **9b** these data indicate that, in contrast to the rhodium complex, the compounds **9a** and **9b** do not contain a significant M−C contact (M = Zn, Hg); the larger value of $^1J(^{13}C,^{31}P)$ is consistent with P−C bond lengths somewhat shorter than those in the rhodium complex (vide infra). The ^{31}P NMR spectra of **9a** and **9b** display singlets with ^{77}Se satellites at 25.4 and 26.0 ppm, respectively. The $^2J(^{31}P,^{31}P)$ and $^1J(^{31}P,^{77}Se)$ coupling constants are somewhat smaller than those in Li**8a**, indicating a small change in the geometry of the PCP unit and slightly stronger M−Se contacts in **9a** and **9b**, resulting in longer P−Se bonds (vide infra). Due to the low solubility of the mercury compound **9b**, only a weak, broad singlet is observed in the ^{199}Hg NMR spectrum instead of the expected quintet arising from the coupling to four equivalent phosphorus atoms. The chemical shift of −793 ppm is, however, comparable with that of the quintet observed at −785 ppm for a related cationic Hg(II) complex of the neutral ligand, {Hg[$H_2C(PPh_2$-$Se)_2]_2$[$ClO_4]_2$}.[31] In addition, doublets are visible at −124 and −82 ppm in the ^{77}Se NMR spectra of **9a** and **9b**, respectively, both at somewhat lower field than the corresponding signal for Li**8a**.

As illustrated in Figure 3, the molecular structures of **9a** and **9b** display the expected Se,Se′ chelation of the anions to the metal center, affording a distorted-tetrahedral environment for the group 12 metals. While the zinc complex **9a** exhibits a centrosymmetric arrangement of the ligands, the symmetry center in the mercury compound **9b** is located between the molecules in the crystal lattice, resulting in different crystal systems for the two compounds. As indicated by the NMR spectra, neither of

(31) Bond, A. M.; Colton, R.; Ebner, J. *Inorg. Chem.* **1988**, *27*, 1697.

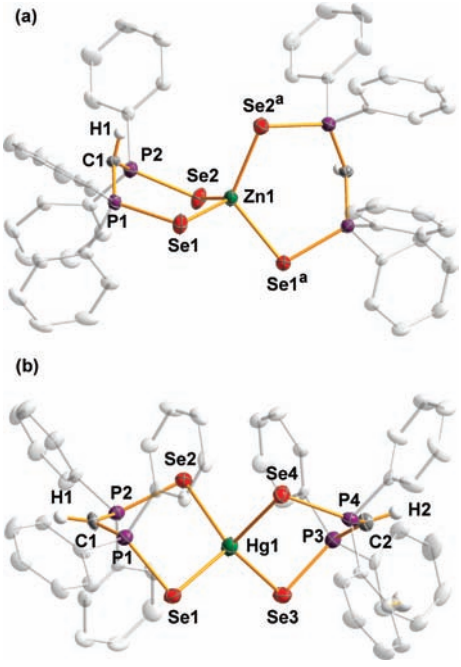

Figure 3. Crystal structures of (a) {Zn[HC(PPh$_2$Se)$_2$]$_2$} (**9a**) and (b) {Hg[HC(PPh$_2$Se)$_2$]$_2$} (**9b**). Hydrogen atoms in the phenyl groups have been omitted for clarity. Symmetry operation: (a) $-x$, y, $0.5 - z$.

the complexes show a significant M−C contact (M = Zn, Hg). Interestingly, however, the CH unit in the PCP region in the zinc compound **9a** is bent toward the metal center, resulting in a boat conformation for the ZnSePCPSe six-membered ring and a significant distortion from planarity for the carbon atom ($\sum\angle$C1 352°; Table 4). In contrast, the planar CH unit in **9b** is pointed away from the metal center and the analogous six-membered ring is notably twisted, as manifested by the dihedral M−Se−P−C angles (Table 4): cf. the pseudoboat conformation observed in the comparable diselenoimidodiphosphinate complexes {M[N(PR$_2$Se)$_2$]$_2$} (M = Zn, R = ^{i}Pr, Ph;[30d] M = Hg, R = ^{i}Pr,[30e] Ph).[32] Since the disparity in the ring conformations for **9a** and **9b** is not apparent in the solution NMR spectra, we attribute this structural difference to crystal-packing effects resulting from the influence of the different orientations of phenyl groups in the two metal complexes on the PC(H)P unit, rather than the difference in size between the two metals or electronic factors. This view is supported by the structures of zinc(II) and mercury(II) halide complexes of the corresponding neutral ligand [H$_2$C(PPh$_2$Se)$_2$].[33,34] In all of these compounds the PCP unit is bent toward the metal center, affording a boat conformation similar to that obtained for **9a**.

Consistent with the lower (by 75−85 Hz) values of $^1J(^{31}P,^{77}Se)$, the P−Se bonds in **9a** and **9b** are ca. 0.04 Å longer than those in the lithium reagent Li**8a**; the P−C bond lengths in **9a**, **9b**, and Li**8a** are equal. In the structure of **9b**, the twisted six-membered ring results in disparities of 0.03 and 0.06 Å in the P−Se and Se−Hg bonds, respectively. The M−Se bonds in **9a** and **9b** are, expectedly, ca. 0.05−0.08 Å shorter than those in metal halide complexes of the neutral ligand {ZnI$_2$[H$_2$C(PPh$_2$Se)$_2$]}[33] and {HgX$_2$[H$_2$C(PPh$_2$Se)$_2$]} (X = Br, I),[34] due to the stronger ionic interaction between the anionic ligand and the metal center. As deduced from the values of $^1J(^{13}C,^{31}P)$, the absence of a M−C contact (M = Zn, Hg) in **9a** and **9b** results in P−C bonds somewhat shorter (by ca. 0.05 Å) than those in the rhodium complex {Cp*Rh[HC(PPh$_2$Se)$_2$]ClO$_4$}.[13] The Se−M−Se bond angles at the metal center in both **9a** and **9b** show a similar range of 99−118°, which is somewhat broader than the range of 103−115° observed in the analogous diselenoimidodiphosphinate complexes {M[N(PR$_2$Se)$_2$]$_2$} (M = Zn, R = ^{i}Pr, Ph;[30d] M = Hg, R = ^{i}Pr,[30e] Ph[32]), despite the virtually identical M−Se and P−Se bond lengths. Finally, while the bond angles at the phosphorus atoms are essentially equal in complexes **9** and Li**8a**, the angles at the selenium atoms are somewhat wider in **9a** and **9b**, presumably owing to the longer M−Se bonds.

One-Electron Oxidation of TMEDA·Li[HC(PPh$_2$Se)$_2$] (Li8a) and TMEDA·Li[HC(P^{i}Pr$_2$Se)$_2$] (Li8c) with I$_2$. The one-electron oxidation of Li**8a** with iodine was performed in order to compare the outcome with similar reactions conducted for the isoelectronic N-bridged anions **2**, which produce dimers of the type **3**, [N(PR$_2$E)$_2$]$_2$ (E = Se, Te; R = ^{i}Pr, ^{t}Bu).[5,6] The reaction of Li**8a** with iodine was conducted at −80 °C in THF. A subtle change in the color of the solution from red (unreacted iodine) into *bright cherry* red was observable at ca. −50 °C, and a further change into pale yellow took place at ca. −20 °C. As indicated by the second color change (at ca. −20 °C), the initially formed neutral radical **10a** (cherry red solution) is a thermally unstable, short-lived species. NMR spectroscopy revealed that the final product is [H$_2$C(PPh$_2$Se)$_2$],[22] presumably formed from **10a** via hydrogen abstraction from the solvent (Scheme 3). The same product was also obtained when the oxidation was carried out in toluene, dichloromethane, or diethyl ether.

Subsequently to the somewhat surprising outcome of the one-electron oxidation of Li**8a**, the reaction of the isopropyl derivative Li**8c** with $^1/_2$ equiv of I$_2$ was carried out under the same conditions to determine the effect of changing the substituents on phosphorus and to gain a more direct comparison with the dichalcogenoimidodiphosphinates **2** in which ^{i}Pr and ^{t}Bu substituents were utilized.[5,6] In the case of Li**8c**, the reaction solution showed only a steady darkening of the red color when the temperature was raised; there was no indication of a second color change. However, consistently with the observations for Li**8a**, NMR spectroscopy showed the formation of [H$_2$C(P^{i}Pr$_2$Se)$_2$] as the final product (Scheme 3).

DFT calculations of the neutral radicals **10** were carried out in order to provide (a) a comparison of the composition of the SOMO with that of the isoelectronic radicals [N(PR$_2$E)$_2$]$^{\bullet}$[5,6] and (b) an estimate of the EPR parameters. The DFT-optimized structures of the neutral radicals **10** are depicted in Figure 4 along with the calculated singly occupied molecular orbitals (SOMOs). The minimum geometries found for the Ph- and ^{i}Pr-substituted systems differ significantly with respect to

(32) Garcia-Montalvo, V.; Novosad, J.; Kilian, P.; Woollins, J. D.; Slawin, A. M. Z.; Garcia y Garcia, P.; Lopez-Cardoso, M; Espinosa-Perez, G.; Cea-Olivares, R. *J. Chem. Soc., Dalton Trans.* **1997**, 1025.
(33) Lobana, T. S.; Hundal, R.; Turner, P. *J. Coord. Chem.* **2001**, *53*, 301.
(34) Lobana, T. S.; Hundal, R.; Singh, A.; Sehdev, A.; Turner, P.; Castineiras, A. *J. Coord. Chem.* **2002**, *55*, 353.

Table 4. Selected Bond Lengths (Å) and Angles (deg) in **9a** and **9b**

	9a[a]	**9b**[b]		**9a**[a]	**9b**[b]
M1−Se1	2.4568(7)	2.647(1)	Se3−P3		2.195(3)
M1−Se2	2.4522(5)	2.679(1)	Se4−P4		2.173(3)
M1−Se3		2.615(1)	P1−C1	1.718(2)	1.732(10)
M1−Se4		2.660(2)	P2−C1	1.724(2)	1.717(10)
Se1−P1	2.1937(7)	2.197(3)	P3−C2		1.699(10)
Se2−P2	2.2026(9)	2.161(3)	P4−C2		1.727(9)
Se1-M1-Se2	116.45(2)	110.88(4)	Se3−P3−C2		118.8(3)
Se1-M1-Se3	98.67(3)[d]	114.97(4)	Se4−P4−C2		118.1(4)
Se1-M1-Se4	102.90(3)[e]	108.72(4)	P1−C1−P2	125.1(1)	123.7(6)
Se2-M1-Se3	102.90(3)[d]	112.15(4)	P1−C1−H1	116(2)	118.1
Se2-M1-Se4	118.26(3)[e]	99.13(4)	P2−C2−H1	111(2)	118.1
Se3-M1-Se4	116.45(2)[d,e]	109.79(4)	P3−C2−P4		128.6(6)
M1−Se1−P1	99.06(2)	91.67(7)	P3−C2−H2		115.7
M1−Se2−P2	101.06(4)	96.40(7)	P4−C2−H2		115.7
M1−Se3−P3		94.98(7)	M1−Se1−P1−C1	19.8(1)	71.2(4)
M1−Se4−P4		101.00(7)	M1−Se2−P2−C1	8.1(1)	63.7(4)
Se1−P1−C1	119.52(8)	117.7(3)	M1−Se3−P3−C2		65.8(4)
Se2−P2−C1	118.27(9)	116.5(3)	M1−Se4−P4−C2		50.9(4)

[a] M = Zn. [b] M = Hg. [c] Symmetry operation: $-x, y, 0.5 - z$. [d] Se3 = Se1[c]. [e] Se4 = Se2[c].

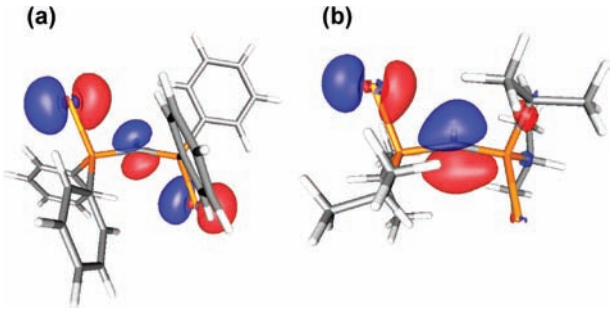

Figure 4. Geometries and SOMOs of the neutral radicals $[HC(PR_2Se)_2]^{\bullet}$: (a) R = Ph (**10a**); (b) R = ^{i}Pr (**10c**).

Scheme 3. One-Electron Oxidation of Li**8a** and Li**8c**

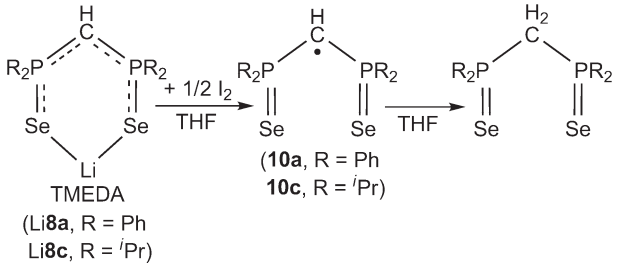

the relative orientation of the phosphorus-bound organic groups that leads to a SOMO consisting of p orbitals either on both or on only one of the selenium centers (**10a** and **10c**, respectively). Most notably, however, the SOMO in both derivatives has a large contribution from the p orbital on the PCP carbon, therefore making it susceptible to hydrogen abstraction. This composition differs from that of the calculated SOMO of the N-bridged systems, $[N(PR_2E)_2]^{\bullet}$, which is almost solely localized on the p orbitals on the two chalcogen atoms E, thus giving rise to formation of the dimers **3**, $[N(PR_2E)_2]_2$, by favorable orbital overlap.[5,6] This disparity in the spatial morphology of the frontier orbitals provides a probable explanation for the preference for hydrogen abstraction over dimerization in the one-electron oxidation of the PCP-bridged anions **8**.

DFT calculations for **10a** and **10c** predict that both radicals will display large (ca. 30 G) hyperfine coupling constants (hfccs) to the two phosphorus nuclei (arising from spin polarization) along with a slightly smaller (16 G) coupling to the −C*H* of the PCP carbon; couplings to the two selenium atoms as well as the PCP carbon are also significant, but they will have only minor contributions to the expected spectra because of the low natural abundance of the ^{77}Se and ^{13}C isotopes. The attempted identification of the transient radicals **10a** and **10c** at low temperature (ca. −40 °C) by EPR spectroscopy was inconclusive. The EPR spectrum of the bright cherry red solution formed upon oxidation of Li**8a** displayed a broad doublet (g = 2.0046) with an hfcc of ca. 11.5 G, while the EPR spectrum of the oxidized solution of Li**8c** exhibited a doublet of binomial triplets at g = 2.0045 with hfccs of 11.3 and 1.6 G, respectively. In view of (a) the *very poor* signal-to-noise ratio for both EPR spectra and (b) the disparity in the experimental and calculated hfccs, no definitive conclusions regarding the identities of the radicals formed upon oxidation of Li**8a** and Li**8c** can be made.[35]

Conclusions

Synthetic routes to the heavy chalcogen-centered anionic ligands $[HC(PPh_2E)(PPh_2)]^-$ and $[HC(PPh_2E)_2]^-$ (E = Se, Te) have been developed. The selenium-containing monoanions $[HC(PPh_2Se)(PPh_2)]^-$ (**7a**) and $[HC(PPh_2Se)_2]^-$ (**8a**) were structurally characterized as Li^+ salts, and the application of the new reagent Li**8a** in metathetical reactions was exemplified by the preparation of the homoleptic group 12 complexes $M[HC(PPh_2Se)_2]_2$ (M = Zn, Hg). In contrast, the tellurium congeners Li**7b** and Li**8b** are thermally unstable.

(35) A reviewer has pointed out that the magnitude of ^{31}P hfccs is markedly dependent on ring torsion angles in certain heterocyclic P(V) radicals.[36] In the current case, however, it seems unlikely that the discrepancy between the calculated and experimental ^{31}P hfccs can be attributed to a conformational change, i.e. bond rotation, since the calculated values for **10a** and **10b** differ by only a few Gauss despite their significantly different conformations.

(36) See, for example: Bestari, K. T.; Cordes, A. W.; Oakley, R. T. *J. Chem. Soc., Chem. Commun*. **1988**, 1328.

Consequently, although the solid-state structure of the monotelluro anion Li**7b** was determined, its use as a reagent is limited to in situ reactions.

The outcome of the one-electron oxidation of the monoanions $[HC(PR_2Se)_2]^-$ (**8**; R = Ph, ^{i}Pr) revealed somewhat surprising differences compared to the analogous reactions with the isoelectronic N-bridged anions, $[N(PR_2E)_2]^-$ (**2**, E = S, Se, Te, R = ^{i}Pr, ^{t}Bu). In contrast to the dimerization processes observed upon oxidation of **2**, the treatment of **8** with iodine produces $[H_2C(PR_2Se)_2]$ (R = Ph, ^{i}Pr) via hydrogen abstraction. This difference in behavior is attributed to the strong contribution from a p orbital on carbon to the SOMO of $[HC(PR_2Se)_2]^{\bullet}$.

Acknowledgment. We gratefully acknowledge financial support from the Academy of Finland and the Natural Sciences and Engineering Research Council (Canada).

Supporting Information Available: CIF files giving X-ray crystallographic data. This material is available free of charge via the Internet at http://pubs.acs.org.